Synthesis of nanostructured Nickel compounds on conductive metallic substrates

J.G. Portillo, J.F. Hernández-Paz, M. Gomez-Mares, I. Olivas-Armendariz, C.A. Rodriguez González *

Instituto de Ingeniería y Tecnología, Universidad Autónoma de Ciudad Juarez, Avenida del Charro No. 450 Norte, 32310 Ciudad Juarez, Chihuahua, Mexico

ARTICLE INFO

ABSTRACT

Nickel hydroxide, oxide, and sulfide films were synthesized on conductive Ni metallic substrates by solid-vapor reactions, calcination and hydrothermal methods. The synthesized films were characterized by XRD, XPS, FE-SEM, UV–Vis Spectroscopy and Cyclic Voltammetry (CV). The morphological analyses of $Ni(OH)_2$ and NiO films showed flower-like nanostructures with thicknesses from 20 to 40 nm; meanwhile the NiS films exhibits nano-granular morphology. All films showed high optical reflectance in the visible region and a sharp absorption edge below 400 nm. The specific capacitance of the Nickel compound ranges from 134 to 311 mF cm^{-2} (at 20 mV s^{-1}) suggesting potential as conductive electrodes for energy storage and electrochemical conversion cells.

© 2019 Elsevier B.V. All rights reserved.

1. Introduction

The increasing demand for high efficiency and low-cost renewable energy technologies has led to developing nanostructured transition-metal materials with promising applications in solar energy conversion, optoelectronics, and energy storage [1,2]. Due to their excellent catalytic properties, and photo-electrochemical stability, Nickel hydroxides, oxides, and sulfides are considered attractive low-cost materials for applications such as fuel cells, batteries, and photovoltaics [3–5].

Nickel hydroxides, oxides, and sulfides nanostructured materials have been synthesized using various top-down routes, including sol-gel, chemical precipitation, hydrothermal, spray pyrolysis, electrochemical process, and chemical vapor deposition [6,7]. However, new studies have followed a more convenient bottom-up approach, in which 1D/2D patterns and morphologies grow in a vertical fashion forming geometrical nano-arrays with higher surface area, thus resulting in more photo-catalytic sites [8]. Some challenges are to overcome the poor conductivity of the Nickel inorganic compounds, which limits its practical applications and to improve the contact between the material and the substrate. Many aqueous chemicals and high-temperature vapor deposition methods over metallic Nickel substrates have been developed [9]. The present work focuses on the synthesis of $Ni(OH)_2$ nano-arrays over metallic Ni substrates by a low-temperature solid-

vapor reaction, and its function as precursor of nano-structured NiO and NiS compounds by high-temperature annealing, and hydro-sulfuration processes, respectively. The correlation between morphologies, electrical conductivity and optical properties for $Ni(OH)_2$, NiO, and NiS were determined.

2. Experimental

A low-temperature solid-vapor reaction was used for the synthesis of $Ni(OH)_2$ nano-flowers or nano-arrays on pure Nickel substrates. Pure one square centimeter Nickel substrates (99.99% Ted Pella Nickel Target – 0.1 mm) were placed inside a sealed autoclave with three beakers containing: 30 mL of $NH_4(OH)$ solution (Alfa Aesar, 28% NH_3), 30 mL deionized water and 2 g of sublimed Sulfur (S) powder (Alfa Aesar, −325 mesh, 99.5%), during 12, 24, 36, 48 and 60 h at 90 °C to promote an even Nickel Hydroxide coating over the metallic surface. The metallic substrates did not have direct contact with the chemical solution during the tests. After cooling to room temperature, the substrates were washed with deionized water and dried. Then, they were annealed and oxidized in an air atmosphere with a muffle furnace at 450 °C for one hour to promote the formation of Nickel Oxide coating over the metallic substrate. The Nickel Sulfide conversion took placed by a solvothermal method when the Nickel Hydroxide phase was exposed to a 0.5 M Sodium Sulfide (Na_2S) solution inside a sealed beaker during 60 min. at 60 °C.

Nickel compounds morphologies, sizes, and film thicknesses were determined by field emission scanning electron microscopy

---

* Corresponding author.
E-mail address: claudia.rodriguez@uacj.mx (C.A. Rodriguez González).

(FESEM). Film thicknesses determination was conducted on at least three cross-sectioned polished samples. Crystalline structures over metallic Ni substrates were characterized in a Rigaku Ultima III X-Ray diffractometer using CuKα radiation. Photoelectron spectroscopy (XPS) analysis was performed using a Thermo Fisher Scientific Inc. photoelectron spectrometer with a monochromatized K-Alpha X-Ray source. Optical reflectance (R) was determined by using an Ocean Optics UV–Vis spectrophotometer with an integrating sphere. Measurements were taken in the wavelength range from 300 to 1000 nm. The optical band gap energies (E_g) were estimated by using the Kubelka-Munk method by plotting $(F(R).h\nu)^2$ versus $h\nu$. The Kubelka-Munk function $F(R)$ was calculated from the recorded reflectance (R) spectra using $F(R) = (1 - R)^2/2R$ equation. Electrochemical properties were determined by a CS350 electrochemical workstation (Wuhan CorrTest Instruments Corp., Ltd.) on a three-electrode cell configuration: synthesized samples (24 h) as working electrodes, Pt foil counter-electrode, and a saturated calomel electrode (SCE) as reference inside a 2 M KOH electrolyte. The specific capacitance was calculated by $C = \int IdE/2A\nu\Delta E$ where $\int IdE$ is the integrated area of the curve of CV, ν is the scanning speed, ΔE is the voltage window, and A is the surface area of the samples.

3. Results and discussion

The Ni substrates exposed (after 24 h) to the solid-vapor reaction showed a fully covered surface by a homogenous green compound film, with excellent adherence (Fig. 1a). The XRD pattern of the green Ni compound (Fig. 1d) identified the film crystalline phase as hexagonal β-Ni(OH)$_2$ (JCPDS#14-0117) with main diffraction peaks at 2θ of 19.25°(0 0 1), 33.02°(1 0 0), 38.49°(1 0 1), 58.94°(1 1 0) and 62.63°(1 1 1). Additional diffraction peaks at 44.2°(1 1 1) and 53°(2 0 0) corresponds to the pure Nickel substrate (JCPDS#04-0850). β-Ni(OH)$_2$ film thickness measurements after exposure to the solid-vapor reaction are shown in Table 1, where the values vary from 4.79 to 59.96 μm at 12 and 60 h, respectively. Conductive Ni substrates exposed to the solid-vapor reaction during 24 h were oxidized at high temperature, forming

Table 1
Reaction time effect on Ni(OH)$_2$ films thicknesses.

Reaction time (hours)	Precursor crystalline phase	Film thickness (microns)
12 h	β-Ni(OH)$_2$	4.79 ± 1.22
24 h	β-Ni(OH)$_2$	10.07 ± 1.26
36 h	β-Ni(OH)$_2$	13.83 ± 1.67
48 h	β-Ni(OH)$_2$	18.62 ± 2.01
60 h	β-Ni(OH)$_2$	59.96 ± 5.18

a black color film, as shown in Fig. 1b. Fig. 1c shows the XRD pattern after the oxidation process, which identified the crystalline phase as cubic NiO with its main diffraction peaks at 37.1°(1 1 1), 43.3°(2 0 0), 62.8°(2 2 0) (JCPDS#47-1049). Exposure of the Nickel substrate covered with Ni(OH)$_2$ by a Na$_2$S solvothermal method, the XRD precursor substrate showed the formation of gray compound (Fig. 1c) which was identified as α and β NiS showing the characteristic peak of both compounds (β-NiS JCPDS#12-0041; α-NiS JCPDS#02-1280). The predominant phase was the low-temperature rhombohedral β-NiS phase with residual hexagonal α-NiS (NiS$_{1.03}$), indicating that the β phase was thermodynamically favored during the solvothermal reaction.

Fig. 2a–c show the FESEM-images of the precursor morphology β-Ni(OH)$_2$ film after 24 h of the solid-vapor reaction. The Nickel compound showed a homogenous distribution of plate-like shapes due to its hexagonal crystalline structure. The morphology of the Nickel Hydroxide shows flowerlike structures composed by smooth flake-like nano-petals with thicknesses from 20 to 40 nm. The nano-flowerlike structures showed good agreement with reported data after 12 h in solvothermal approaches [10]. Flower-shaped NiO structures composed of thin nano-petals were also obtained by thermal decomposition at 450 °C of precursor β-Ni(OH)$_2$ samples in air. Fig. 2d–f show how the NiO morphologies are like the ones observed in the Nickel Hydroxide structures with flake-like nano-petals and thicknesses from 20 to 40 nm. Fig. 2g–i shows the film morphologies of the substrates covered with the Nickel Sulfide compound. The compound shows a nano-granular morphology, indicating how the Ni(OH) precursor morphology changed.
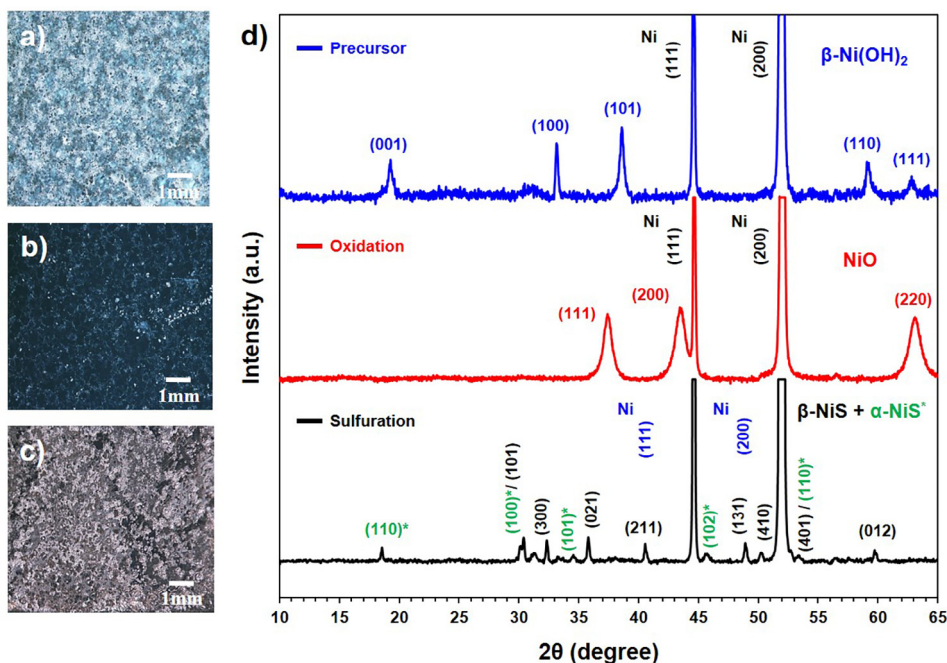
Fig. 1. Synthesized films over metallic Ni: a) as-prepared Ni(OH)$_2$ precursor, b) NiO film, c) NiS film, and d) Ni films XRD patterns.
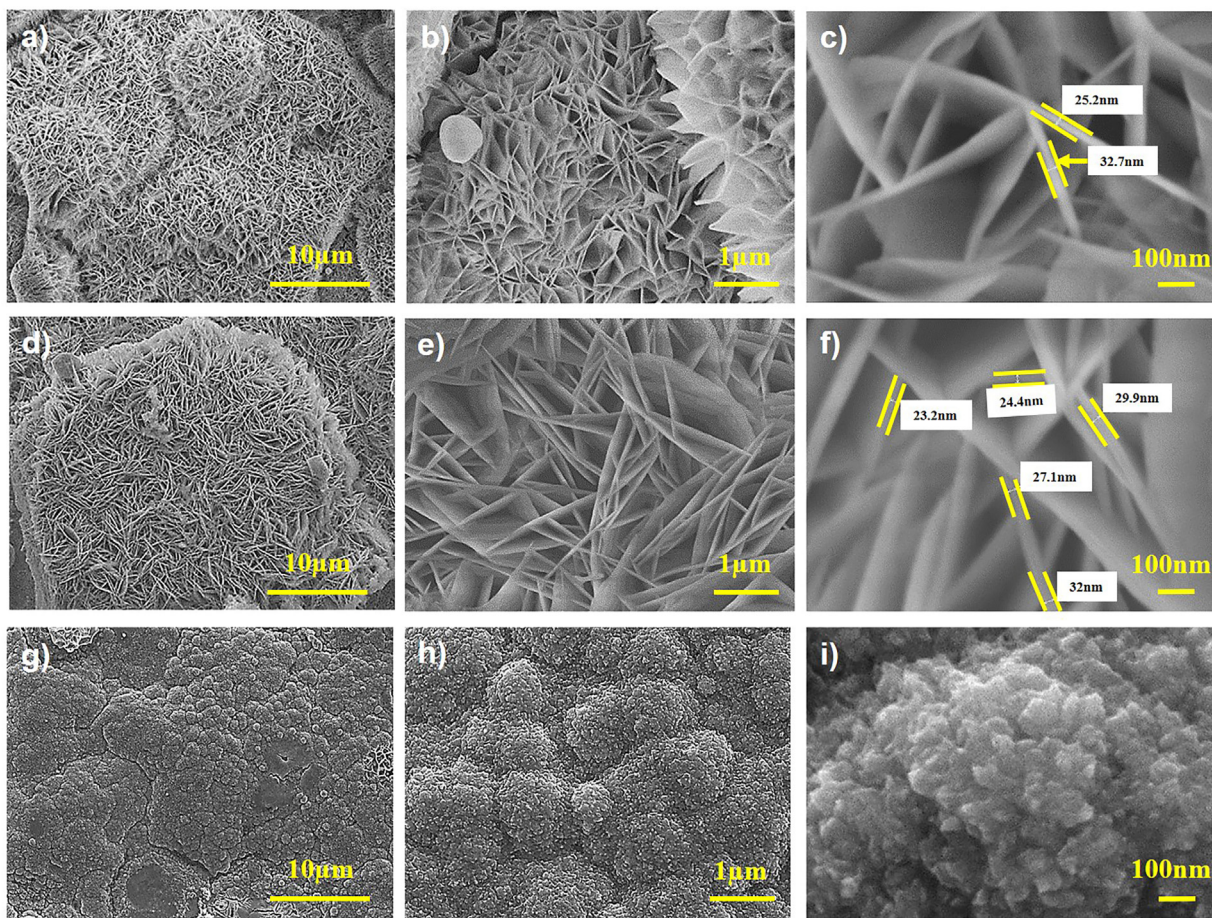
Fig. 2. FESEM-images of: a–c) as-prepared Ni(OH)$_2$ nanostructured films precursor, d–f) NiO nanostructured films morphology, and g–i) NiS films granular morphology.
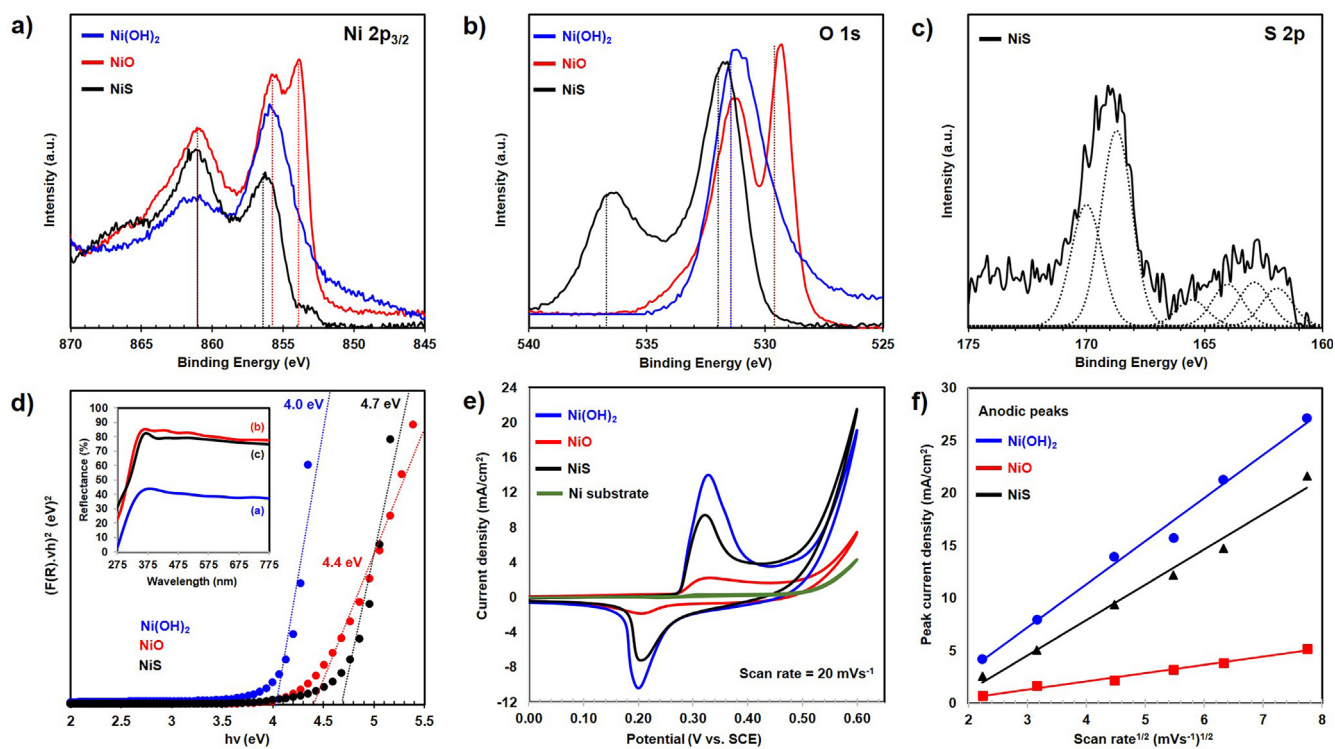

Fig. 3. XPS analyses (a–c), band-gaps (d) and cyclic voltammetry (e,f) of the synthesized films.

XPS was performed to determine the surface chemical composition. The XPS spectra of the $Ni(OH)_2$ (Fig. 3a) precursor showed the main Ni-$2p_{3/2}$ peak at 855.6 eV with a satellite peak near 861 eV that corresponds to $Ni(OH)_2$ characteristic binding energy peaks. Oxidized precursor sample showed a main binding energy peak at 853.8 eV that corresponds to NiO. However, the characteristic $2p_{3/2}$ binding energy peaks of $Ni(OH)_2$ are also present in the outside layer, which indicates a reaction of the NiO substrate with the air and humidity present in the air. In the same way, the outer sulphurated NiS layer showed a binding peak at 856.5 eV, where $NiSO_4$ binding energy values have been reported, with a broad satellite peak near 861 eV related to OH^- species. XPS O-1s spectrum (Fig. 3b) of the oxidized substrate fitted with two peaks, one at a binding energy of 524.4 eV and the second at 531.2 eV. The first peak is located in the NiO binding energy range from 529 to 530 eV, whereas the latter indicates the presence of a $Ni(OH)_2$ compound (531–532 eV) attributed to the hydroxyl group chemisorbed to the NiO surface. The O-1s spectra of the sulfurized substrate confirmed the presence of a $NiSO_4$ layer by showing a broad binding peak at 531.8 eV which indicates a possible degree of hydration by containing hydroxy Nickel species. Fig. 3c shows S-2p spectra of the sulphurated substrate, the binding energy peak 168.5 eV related to the $NiSO_4$ layer, and multiple polysulfide peaks from 162 to 164 eV. It has been reported that near-surface sulfide species, including other sulfide ions, may lead to the formation of polysulfides in NiS compounds exposed to air and high humidity conditions.

The (a) $Ni(OH)_2$ nano-flowerlike, (b) NiO nano-flowerlike and (c) NiS irregular morphologies were characterized by diffuse reflectance in the UV–Vis region from 300 to 800 nm (Fig. 3d). The NiO and NiS films exhibit an 80% reflectance in the visible, and the near IR regions, meanwhile the $Ni(OH)_2$ showed a lower reflectance at the same wavelength regions. All Nickel compounds showed absorption edges below 400 nm, in the near-ultraviolet area. Fig. 3d displays the calculated band gaps of each Nickel compound. The E_g values were 4.1 eV for the $Ni(OH)_2$, 4.5 eV for the NiO, and 4.8 eV for the NiS thick films. The lower E_g value of the $Ni(OH)_2$ could be related to the chemical composition and the smaller crystallite size.

Fig. 3e represents the Ni-compounds cyclic voltammetry curves at a scan rate of 20 mV s^{-1} in the potential range of -0.2 to 0.6 V (vs. SCE). The three materials exhibit a battery-type Faradaic reaction with redox peaks. The larger integral area is observed in the $Ni(OH)_2$ films when compared with the NiS and NiO, which implies a larger specific capacitance. The specific capacitances of the $Ni(OH)_2$, NiS, and NiO samples were found to be 311, 262 and 134 mF cm^{-2} respectively at the scan rate of 20 mV s^{-1}. Fig. 3f shows anodic peak current vs. the square root of scan rate. All sample possess a well fitted linear relationship suggesting that the process is under diffusion control. The slope of $Ni(OH)_2$ electrode is larger than the others, suggesting a more favorable ion diffusion.

4. Conclusions

β-$Ni(OH)_2$, NiO and NiS films over a conductive Nickel substrate were prepared by different synthesis techniques. Homogenous β-$Ni(OH)_2$ films were obtained after 24 h of solid–vapor reaction. XRD results indicated the presence of NiO and NiS films after exposure of the precursor $Ni(OH)_2$ film to a high-temperature annealing process, and low-temperature solvothermal method respectively. The surface morphological variations of the Nickel compounds were displayed by FESEM indicating the presence of nano-flowers in the Nickel hydroxide and oxide compounds. XPS surface analysis showed that NiO and NiS substrates were susceptible to hydration and/or oxidation by forming $Ni(OH)_2$ and $NiSO_4$ compounds in the outer layers. The deposited Nickel compound films showed high optical reflectance in the visible region and exhibited a sharp absorption edge below 400 nm in the near UV region, where the $Ni(OH)_2$ showed the lowest band-gap (4.1 eV). The cyclic voltammetry results showed specific capacitance of 311, 262 and 134 mF cm^{-2} (scan rate of 20 mV s^{-1}) for the $Ni(OH)_2$, NiS, and NiO samples showing potential as conductive electrodes for energy storage and electrochemical conversion cells.

Declaration of Competing Interest

The authors declare that they have no known competing financial interests or personal relationships that could have appeared to influence the work reported in this paper.

Acknowledgment

References

[1] M. Gao, Y. Xu, J. Jiang, S. Yu, Chem. Soc. Rev. 42 (2013) 2986–3017.
[2] T. Guo, M. Yao, Y. Lin, C. Nan, CrystEngComm 17 (2015) 3551–3585.
[3] J. Theerthagiri et al., Nanomaterials 8 (2018) 256.
[4] R.S. Kate, S.A. Khalate, R.J. Deokate, J. Alloys Compd. 734 (2018) 89–111.
[5] M. Moniruzzaman, C.Y. Yue, K. Ghosh, R.K. Jena, J. Power Sources 308 (2016) 121–140.
[6] D.S. Hall, D.J. Lockwood, C. Bock, B.R. MacDougall, Proc. R. Soc. A 471 (2015) 2174.
[7] N.K. Chaudhari, H. Jin, B. Kim, K. Lee, Nanoscale 9 (2017) 12231.
[8] B. Ni, X. Wang, Adv. Sci. 2 (2015) 1500085.
[9] A. Montebelli et al., Catal. Sci. Technol. 4 (2014) 2846.
[10] N. Parveen, M.H. Cho, Sci. Rep. 6 (2016) 27318.